Supercond. Sci. Technol. **22** (2009) 095011 (4pp) doi:10.1088/0953-2048/22/9/095011

Effects of disorder on the superconducting properties of $BaFe_{1.8}Co_{0.2}As_2$ single crystals

M Eisterer[1], M Zehetmayer[1], H W Weber[1], J Jiang[2], J D Weiss[2], A Yamamoto[2] and E E Hellstrom[2]

[1] Atominstitut, Vienna University of Technology, Austria
[2] National High Magnetic Field Laboratory, Florida State University, Tallahassee, FL 32310, USA

Received 20 May 2009, in final form 22 June 2009
Published 5 August 2009
Online at stacks.iop.org/SUST/22/095011

Abstract
Single crystals of superconducting $BaFe_{1.8}Co_{0.2}As_2$ were exposed to neutron irradiation in a fission reactor. The defects introduced decrease the superconducting transition temperature (by about 0.3 K) and the upper critical field anisotropy (e.g. from 2.8 to 2.5 at 22 K) and enhance the critical current densities by a factor of up to about 3. These changes are discussed in the context of similar experiments on other superconducting materials.

(Some figures in this article are in colour only in the electronic version)

1. Introduction

Neutron irradiation is a powerful tool for theoretical studies as well as the optimization of superconductors [1–9], since electron scattering centers and/or pinning sites are introduced. The effects can be investigated on the same sample allowing comparisons with theoretical predictions for changes in inter and intraband scattering [1, 7, 8] or with pinning models for uncorrelated, randomly distributed, nano-sized pinning centers [3, 5–7]. Scattering seems to be particularly interesting in the FeAs based materials since they are multi-band superconductors, possibly with (presently still unexplored) extended s-wave pairing symmetry [10]. The changes in scattering and pinning also provide guidelines for material optimization.

2. Experimental details

The $BaFe_{1.8}Co_{0.2}As_2$ crystals (typically $1.4 \times 0.7 \times 0.1$ mm^3) were prepared by the self-flux method [11] at the National High Magnetic Field Laboratory and irradiated at the Atomic Institute to a fast neutron fluence of 4×10^{21} m^{-2}. Defects are introduced either by direct collisions of high energy neutrons with lattice atoms or by nuclear reactions. All nuclei can capture neutrons followed by a prompt gamma emission of a few MeV. The recoil energy is sufficient to displace the emitting nucleus. The same holds for the β-decay of ^{76}As. However, many of the resulting Frenkel pairs recombine quickly and the stable defects add to those produced by direct collisions, whose density is also unknown. Larger defects can be created only by fast neutrons ($E > 0.1$ MeV).

One crystal was mounted onto a rotating sample holder and investigated in a superconducting 17 T solenoid. A current of 300 μA ($\sim$3 kA m^{-2}) was applied in order to measure resistivity at various angles and magnetic fields while cooling at a rate of 10 K h^{-1}. The upper critical field was evaluated using three different criteria: 90% (onset), 50% (midpoint), and 10% (offset) of the normal state resistivity, which was extrapolated linearly from its behavior just above the transition temperature. The transition width, ΔT_c, refers to the temperature difference between the onset and the offset. All results refer to the 50% criterion in the following, although the same analysis was also made on the basis of the 90% and 10% criteria. No qualitative influence on the results was found (cf figure 4), but data scattering was smallest for the 50% criterion, since the transition is steepest there.

A second crystal was characterized magnetically. Its transition temperature was measured in a SQUID using ac-mode with a field amplitude of 0.1 mT. Irreversible properties were studied from magnetization loops— $m(H_a)$—with $H_a \parallel c$ measured in a VSM at fields up to 5 T and a field sweep rate of 10^{-2} T s^{-1}. The critical current density, J_c, was evaluated by applying Bean's model for rectangular samples (e.g. [5]).

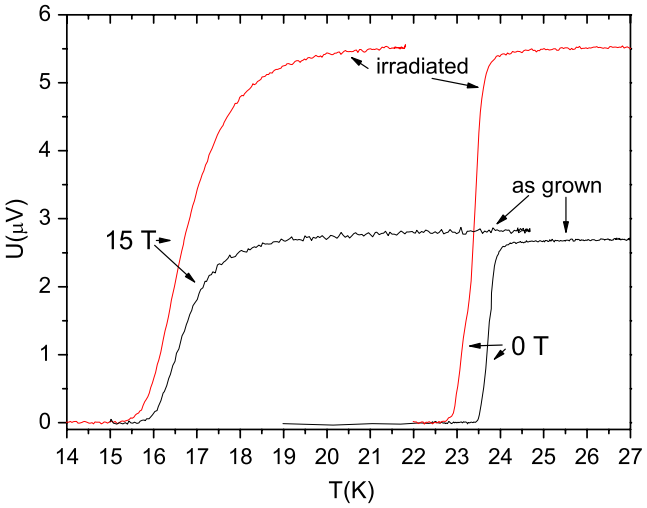

Figure 1. Resistive transitions at 0 and 15 T ($B \parallel c$) prior to and after neutron irradiation.

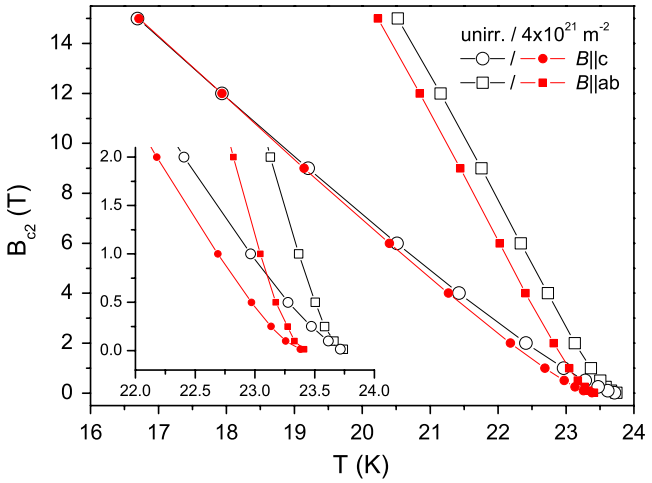

Figure 2. The upper critical field, for the two main field orientations, $B_{c2}^{\perp}(T)$ and $B_{c2}^{\parallel}(T)$. The irradiation increases the slope only for $B \parallel c$.

3. Resistivity and transition temperature

The transition temperature was found to be 23.75 K with a small transition width of 0.35 K (figure 1), increasing to only about 1.5 K at 15 T ($B \parallel c$, perpendicular to the FeAs layers). T_c decreased to 23.4 K after irradiation and ΔT_c at zero field increased to 0.6 K. The decrease in T_c was confirmed by ac susceptibility measurements on the second crystal, from $\simeq$23.4 to 23.1 K. A decrease in T_c was recently predicted to result from impurity scattering in extended s-wave superconductors [12]. However, the decrease in T_c after neutron irradiation is a rather common feature observed in many different materials, such as the cuprates [2, 6], MgB_2 [7] and the A-15-compounds [1], since it can also be caused by d-wave superconductivity [13], interband scattering [8], a change in the electronic density of states [8] or by a reduction in anisotropy [13].

An enhanced density of impurity scattering centers after neutron irradiation is evidenced by the residual resistivity ratio, RRR $= \rho_n(300\ \mathrm{K})/\rho_n(25\ \mathrm{K})$, which decreases from 2.2 to 1.9. Since the resistivity is only weakly temperature dependent above T_c, $\rho_n(25\ \mathrm{K})$ represents a reasonable estimate for the residual resistivity ρ_0, which seems to increase by a factor of about 2 in figure 1. We did not calculate the absolute values of the resistivity due to large uncertainties in the determination of the crystal geometry. Also the absolute change in voltage is not reliable since we did not use the same contacts before and after irradiation, therefore, the distance between the voltage taps slightly changed and could not be determined exactly because of the finite contact area. Only the RRR is independent of the actual geometry.

4. Upper critical field and anisotropy

The upper critical field for both main field orientations is plotted as a function of temperature in figure 2. While $B_{c2}^{\parallel}(T)$ (field parallel to the *ab* planes) shifts to lower temperatures without a significant change in slope, $B_{c2}^{\perp}(T)$ becomes steeper after irradiation leading to an enhancement at low temperatures. This is expected from a reduction of the electron mean free path due to impurity scattering in s-wave superconductors. In d-wave superconductors a *decrease* of B_{c2} is predicted theoretically [14]. We are not aware of the corresponding prediction for extended s-wave pairing.

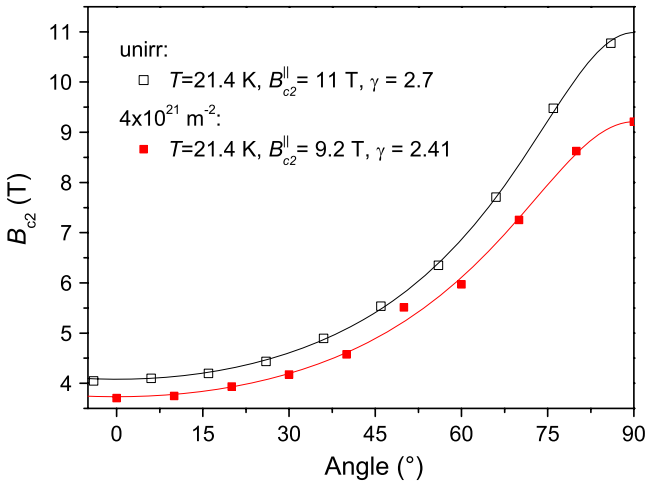

Figure 3. The angular dependence of the upper critical field agrees with the prediction of anisotropic Ginzburg Landau theory (solid lines) prior to and after the irradiation.

The angular dependence of the upper critical field is plotted in figure 3. $B_{c2}(\theta)$ at a fixed temperature was obtained from linear interpolation between the values measured at fixed fields (cf figure 2). This does not induce a significant systematic error, since the curvature of $B_{c2}(T)$ is small except for a small temperature region near T_c, where the number of measured points was high anyway.

The data are in excellent agreement with anisotropic Ginzburg Landau theory, $B_{c2}(\theta) = B_{c2}^{\parallel}(\gamma^2 \cos^2(\theta) + \sin^2(\theta))^{-0.5}$. The upper critical field anisotropy, γ, was determined by fitting this relation to the experimental data. The anisotropy has a maximum of 2.9 at 22.8 K, which is reduced to

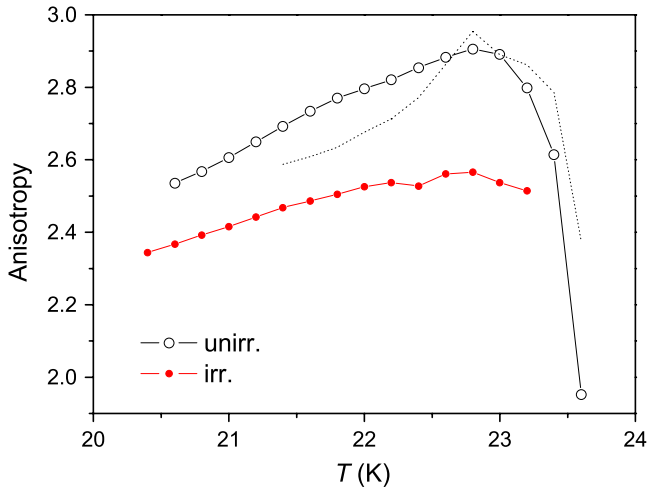

Figure 4. The upper critical field anisotropy increases with temperature, except in the close vicinity of T_c. The irradiation reduces the anisotropy. Dotted line graph represents $\gamma(T)$ of the as-grown sample evaluated by the 90% criterion for comparison. (The other data refer to the 50% criterion.)

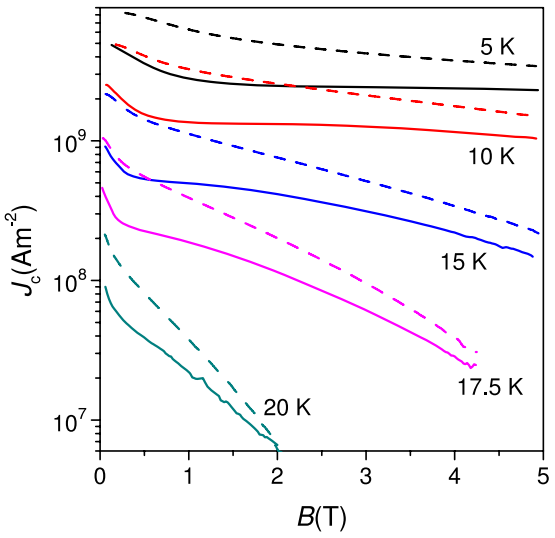

Figure 5. Critical current density within the *ab* plane before (solid lines) and after (dashed lines) neutron irradiation as a function of magnetic induction.

2.55 after irradiation (figure 4). A reduction in γ upon neutron irradiation was also found in the cuprates [6] and in MgB_2 [7]. The pronounced drop of γ near T_c can be directly observed in the inset of figure 2 and is obviously related to the curvature of $B_{c2}(T)$.

The anisotropy agrees with previous reports [15–17]. The present experiment demonstrates that γ is sensitive to impurity scattering, which will result in sample to sample variations. Note that electron scattering by the doping atoms (Co in this case) cannot explain the doping dependence of the anisotropy, since an increase of γ was found at higher concentrations of doping atoms [15].

5. Critical currents

The critical current densities, $J_c(B)$, obtained from magnetization measurements at temperatures from 5 to 20 K are presented in figure 5 (solid lines) and confirm [17] that the major part of the superconducting phase diagram is dominated by irreversible properties, in contrast to many HTSC and LTSC single crystals. This indicates that Ba-122 crystals contain a rather effective as-grown pinning matrix. Very recently, STM investigations of similar crystals [18] revealed impurities with a radius of about 1–2 nm (according to the figures of [18]), which are presumably related to Co or Fe vacancies. Their size would perfectly match to the coherence length of the material (∼2–3 nm) and could therefore provide perfect core pinning. Controlling their density, e.g. during the growth process, could make the material very attractive for applications. After a sharp decay of J_c at low fields, the curves are almost constant over a larger field interval and show traces of a fishtail effect (but no real second maximum—cf figure 5 solid lines). According to theory, the sharp decay at low fields reflects the significant role of the repulsive vortex vortex interaction (i.e. the elastic energy) at that region, whereas the fishtail [19] results from a more pronounced role of the pinning energy at higher fields, which competes with the elastic (vortex) energy and leads to a more disordered lattice and a better adjustment to the defect matrix.

Neutron irradiation enhances J_c—figure 5 (dashed lines). Since the reversible properties are only slightly affected by the chosen neutron fluence, the modification of the pinning matrix seems to be mainly responsible for these effects. Neutron irradiation is known to introduce very effective pinning centers in a wide range of superconducting materials including the cuprates like Y-123 [2] and MgB_2 [5], where spherical defects with a size comparable to the coherence length are introduced. The pronounced J_c enhancement in Ba-122 suggests a similar defect generation, but note that the enhancement is smaller than in many other single crystals. This is in agreement with our assumption of a rather effective as-grown defect matrix (compared to other materials), since the relative effect of strong (radiation induced) pinning centers is expected to be larger in very clean samples [4]. For instance, Y-123 exhibits a strongly temperature dependent enhancement [4] by up to a factor of 100 at high temperatures (e.g. at 77 K) and roughly 4–5 at low temperatures (5 K, all data refer to low fields) which can be explained by the thermal fluctuations and the more two-dimensional character at high temperatures. The enhancement in MgB_2 single crystals [5] was found to be about 5–7 at low fields and to remain quite constant over the temperature range.

The results on Ba-122 are presented in figure 6. The enhancement of the critical current density $J_{c,irr}/J_{c,unir}$ lies between about 3 and 1. Like in MgB_2 there is only a weak temperature dependence, which suggests that both the as-grown and the radiation induced pinning sites are not much smaller than the coherence length, since very small pinning sites would be effective only at low temperatures, where the coherence length is small and the thermal energy negligible. The traces of the fishtail effect observed in the as-grown state disappear upon irradiation indicating that the new pinning sites transfer the ordered vortex lattice at

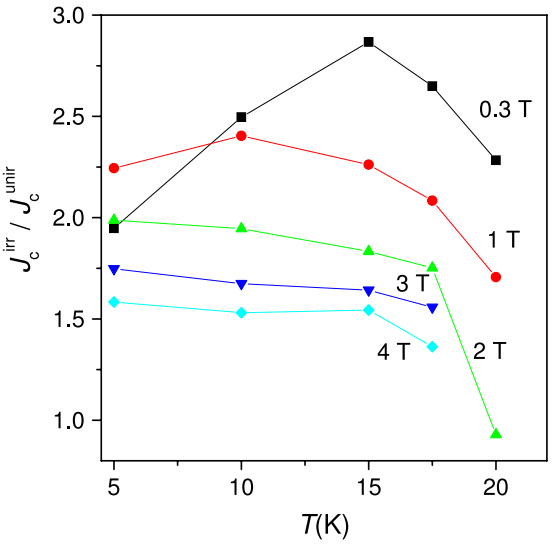

Figure 6. Ratio of critical currents before (J_c^{unir}) and after (J_c^{irr}) neutron irradiation as a function of temperature at various applied fields.

low fields into a pinning dominated disordered phase. This behavior agrees with theory and was found in many HTSC samples upon irradiation [3, 4] and recently also in Sm-1111 [9]. Accordingly, the enhancement is largest at those fields, where the ordered state was mostly pronounced in the unirradiated state. At higher fields, the enhancement decreases and approaches 1 near the irreversibility field in the high temperature measurements (where sufficiently high fields are accessible). Similar effects have been found in many Y-123 and other HTSC crystals, where the irreversibility line is not significantly affected by neutron irradiation.

6. Conclusions

In conclusion, we found that electron scattering increases after neutron irradiation leading to a slight decrease of T_c and the anisotropy. The critical current density increases by a factor of up to 3, indicating that the radiation induced defects are effective pinning centers. These results are in qualitative agreement with our recent study on polycrystalline Sm-1111 [9].

Acknowledgments

We are grateful to D C Larbalestier, A Gurevich, M Putti, D V Abraimov, C Tarantini and F Kametanni for discussions. Work at the NHMFL was supported by AFOSR, NSF, and the State of Florida. Parts of the work at the Atominstitut were supported by the Austrian Science Fund under contract 21194.

References

[1] Sweedler A R, Cox D E and Moehlecke S 1978 *J. Nucl. Mater.* **72** 50
[2] Sauerzopf F M 1998 *Phys. Rev.* B **57** 10959–71
[3] Werner M, Sauerzopf F M, Weber H W and Wisniewski A 2000 *Phys. Rev.* B **61** 14795–803
[4] Zehetmayer M, Sauerzopf F M, Weber H W, Karpinski J and Murakami M 2002 *Physica* C **383** 232
[5] Zehetmayer M, Eisterer M, Jun J, Kazakov S M, Karpinski J, Birajdar B, Eibl O and Weber H W 2004 *Phys. Rev.* B **69** 054510
[6] Zehetmayer M, Eisterer M, Sponar S, Weber H W, Wisniewski A, Puzniak R, Panta P, Kazakov S M and Karpinski J 2005 *Physica* C **418** 73
[7] Krutzler C, Zehetmayer M, Eisterer M, Weber H W, Zhigadlo N D and Karpinski J 2007 *Phys. Rev.* B **75** 224510
[8] Putti M, Brotto P, Monni M, Galleani E, Sanna A and Massidda S 2007 *Eurohys. Lett.* **77** 57005
[9] Eisterer M, Weber H W, Jiang J, Weiss J D, Yamamoto A, Polyanskii A A, Hellstrom E E and Larbalestier D C 2009 *Supercond. Sci. Technol.* **22** 065015
[10] Mazin I I, Singh D J, Johannes M D and Du M H 2008 *Phys. Rev. Lett.* **101** 057003
[11] Sefat A S, Jin R, McGuire Michael A, Sales Brian C, Singh D J and Mandrus D 2008 *Phys. Rev. Lett.* **101** 117004
[12] Bang Y, Choi H-Y and Won H 2009 *Phys. Rev.* B **79** 054529
[13] Millis A J, Sachdev S and Varma C M 1988 *Phys. Rev.* B **37** 4975
[14] Won H and Maki K 1994 *Physica* B **244** 353
[15] Ni N, Tillman M E, Yan J-Q, Kracher A, Hannahs S T, Bud'ko S L and Canfield P C 2008 *Phys. Rev.* B **78** 214515
[16] Tanatar M A, Ni N, Martin C, Gordon R T, Kim H, Kogan V G, Samolyuk G D, Bud'ko S L, Canfield P C and Prozorov R 2009 *Phys. Rev.* B **79** 094507
[17] Yamamoto A *et al* 2009 *Appl. Phys. Lett.* **94** 062511
[18] Yin Y, Zech M, Williams T L, Wang X F, Wu G, Chen X H and Hoffman J E 2009 *Phys. Rev. Lett.* **102** 097002
[19] Mikitik G P and Brandt E H 2001 *Phys. Rev.* B **64** 184514